

GAMMA ATTENUATION THROUGH NANO LEAD – NANO COPPER PVC COMPOSITES

by

**Yehia M. ABBAS¹, Ahmed M. EL-KHATIB², Mohamed S. BADAWI³,
Mahmoud T. ALABSY^{2*}, and Osama M. HAGAG⁴**

¹Department of Physics, Faculty of Science, Suez Canal University, Ismailia, Egypt

²Physics Department, Faculty of Science, Alexandria University, Alexandria, Egypt

³Department of Physics, Faculty of Science, Beirut Arab University, Beirut, Lebanon

⁴Physics Department, Faculty of Science, Port Said University, Port Said, Egypt

Scientific paper

<https://doi.org/10.2298/NTRP210110001A>

Polymer composites of polyvinyl chloride, PVC, were loaded up with micro and nano PbO/CuO particles. The added percentage of each by mass was 10 wt.%, 20 wt.%, 30 wt.%, and 40 wt.%, plus 40 wt.% of mixed composite (20 wt.% CuO + 20 wt.% PbO). The mass and linear attenuation coefficients of the investigated composites were measured as a function of gamma-ray energies going from 59.53 keV to 1408.01 keV utilizing standard radioactive point sources. To confirm the validity of these results the attenuation coefficients for bulk composites (PVC + PbO and PVC + CuO) were calculated by using the XCOM software. The results were in good agreement with the values obtained from the experimental work. By comparing the attenuation coefficients of the different composites it was found that those loaded with either nano PbO or CuO have higher values than those loaded with bulk sizes with the same percentage. Also, samples loaded with nano PbO have the highest attenuation coefficients even by comparing them with (20 wt.% CuO + 20 wt.% PbO), especially in the energy region below 1 MeV, but for greater energies, the values become very closed. The investigation of the mechanical properties of such composites due to the injection of bulk and nano metals reveals that tensile strength and Young's modulus of PVC nanocomposite sheets were notably increased with the increasing concentration of CuO and PbO nanoparticles. The CuO nanocomposite showed the highest values of flexural strength, toughness, and tensile strength among all the fabricated nanocomposite sheets.

Key words: polyvinyl chloride, nano lead oxide, nano copper oxide, characterization, nano lead-copper-PVC composite, gamma-ray, attenuation coefficient, mechanical property

INTRODUCTION

The use of radiation in many fields of our daily life has become a fact that people cannot avoid [1, 2]. It is very important and interesting to study new materials to protect people against radiation and to minimize the pollutants in our environment [3]. Currently, the considering of attenuation of gamma-beams by polymer composites has become an interesting field of research [4]. This is because of the broad utilization of radioactive gamma sources in medication, farming, industry, logical research, and in many applied fields [5]. Gamma-beams present a hazard to living organisms which depends on gamma energy and time. In turn, this leads to consideration of new protective materials that depend on the use of radiation [6].

Consequently, a helpful material as a shield is always critical to saving lives and different materials due to the hazardous effect of these poisonous radiations being emitted from unprotected radioactive sources. The main task of this shield is to reduce the dangerous dose by interfacing the source of radiation as well as the diminishing intensity of radiation [7]. Large atomic number compounds, for instance, Pb blocks, concrete mixed with metals are ordinarily used for that aim [5]. Other metal-based protecting materials for example steel [8], tungsten [9], bismuth [10], and copper [11] so far (have so far been) used as protecting materials. In any case, Pb is exceptional among all these materials due to its great density, low cost, and high atomic weight. However, Pb shows various essential drawbacks that limit its applications and usage, for example: high heaviness, high toxicity, inflexibility, and low chemical stability. To overcome these limitations, polymer composites were widely investigated as alternative radiation-protecting materials.

* Corresponding author; e-mail: mahmoud.alabsy@yahoo.com

Polymers have very low mechanical characteristics but are useful because of their flexibility in applications requiring such a property. They are usually deformed at high strain under loading [12]. During the past years, the major development in polymer science has been enriched by our knowledge of the relationship between the structure of the polymers and their properties. Polymers are ideal materials for many industrial applications because they have desirable properties such as durability, transparency, flexibility, low cost of synthesis, and fabrication of electric and thermal resistance. Mechanical properties such as stiffness, the tensile strength of polymers play a decisive role in industrial applications like extruding operators, implantation of biochemical sensors, and waveguiding layers [12, 13].

MATERIALS AND METHODS

This part explains the preparation steps of both nano PbO and nano CuO plus the composite sheets used in this work.

Preparation of PbO nanoparticles

PbO nanoparticles were synthesized chemically according to the following steps [4]:

- Adding 150 ml of distilled water to 114 g of NaOH then mixed.
- Adding 180 ml of distilled water with 68.1 g of lead acetate and warm at 90 °C in an oven.
- Mix the previous NaOH solution with a lead acetate solution until the red color is obtained.
- Filtrate the precipitate and dry it at 100 °C for 8 hours.
- The dried precipitate has been lightly pounded by an agate pestle (the Mortar Grinder RM 200) and mortar to obtain a yellow precipitate.

Preparation of CuO nanoparticles

CuO nanoparticles were synthesized chemically [14] according to the following steps:

- Adding 15 g ascorbic acid, 2 g CuSO₄ to 100, 50 ml hot water, respectively.
- Then mix them for about 3 minutes and put in an oven at 80 °C for 12 hours.
- The resulting product was removed and lightly pounded by an agate pestle (the Mortar Grinder RM 200) and mortar to obtain a black precipitate.

Synthesis of polyvinyl chloride composites

Polyvinyl chloride (PVC) is a generally utilized plastic material that is one of the most valuable items

for the substance business. In over half of the industrial facility PVC is utilized in development as a development material since it is modest and simple to introduce. Lately, PVC has supplanted numerous development materials in numerous zones despite worries about the effect of PVC on the Earth and human wellbeing [1].

The PVC loaded with 10 wt.%, 20 wt.%, 30 wt.%, and 40 wt.% filler (PbO, CuO) either bulk or nano by weight was fabricated using a pressure forming system. It was prepared according to the following steps:

- Preparing the different mixtures from the PVC powder and filler.
- The mixture as a powder was placed slowly in the pressure forming system to be compressed by two roll mixers at 180 °C for 10 minutes at a speed of 40 rpm to produce a homogeneous soft sample.
- Then the soft sample was poured into a stainless steel mold with dimensions 40 cm × 40 cm and 0.3 cm thickness.
- Using a laser beam the sheet was cut into discs with a diameter of 8.4 cm for studying the attenuation of gamma rays.

Structural characterization

A SEM (JSM- 6010LV, JEOL), was employed to observe the micrographs and the cross-section morphologies of the prepared PVC composites filled with micro and nano PbO/CuO particles. To prepare the samples for SEM observation, the samples were coated with an ultrathin gold coating using a low-vacuum sputtering coating device (JEOL-JFC- 1100E). The SEM micrographs were obtained at a magnification order of 10000 at 20 kV. Moreover, the distribution of the PbO and CuO nanoparticles in the PVC matrix was also analyzed by employing the field emission transmission electron microscope, FE-TEM, (JEM 2100F, JEOL, Japan) at 200 kV.

Mechanical instrumentation

Tensile tests are utilized to measure the stiffness, ultimate tensile strength, percentage of elongation at break, yield stress, and other tensile properties by using the DVT FU/ DLC Tensile/ Compression test device (50 kN). The tensile tests are performed to indicate how the prepared composites will react to forces being applied in tension [15]. The shape of the tensile test specimen is depicted in fig. 1. The test pieces to be used should be 3 mm thick. Generally, the test piece has gripped ends that are wider than the parallel length. The parallel length, L_c , has to be connected to the ends using transition curves with a radius of at least 20 mm and free length between the grips for parallel-sided test piece 140 mm [15].

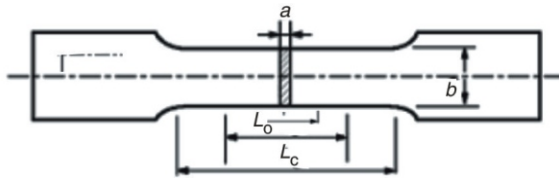


Figure 1. Test specimens shape [15]

Gamma-ray spectroscopy set-up

Five standard radioactive point sources ^{241}Am , ^{133}Ba , ^{137}Cs , ^{60}Co , and ^{152}Eu , purchased from Physikalisch-Technische Bundesanstalt PTB in Braunschweig and Berlin, emitting energies in an interval from 59.53 keV to 1408.01 keV were used in the gamma-radiation measurements. The experimental measurements were carried out using a gamma-ray spectrometer which consists of an (HPGe) hyper pure germanium cylindrical detector well-calibrated from Canberra (Model GC1520), multichannel analyzer, and amplifier (MCA). The relative efficiency of the HPGe detector is 15 % in energy going from 50 keV to 10 MeV with a resolution of 1.85 keV at 1.33 MeV gamma-ray peak ^{60}Co [16]. The HPGe detector placed in a Pb shield of 15 cm thickness and a copper lining on the inside to diminish the background radiations and minimize the X-ray interferences. The experimental arrangement for the gamma measurement system is displayed in fig. 2. The gamma radioactive source was placed at a height of 508.67 mm to get a narrow beam and to minimize the errors due to the dead time and summing effects [17]. The gamma spectra for all measurements were collected for sufficient period of time, according to the sample thickness, so that the statistical error would be less than 1 %. The Genie 2000 program was used to analyze the obtained spectra. The net areas under each peak in the spectrum as a function of energy and thickness were tabulated in an Excel sheet [18].

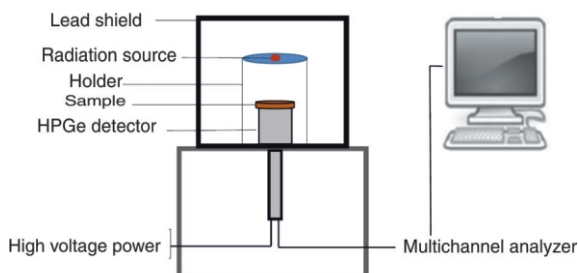


Figure 2. Experimental arrangement for gamma measurement

RESULTS AND DISCUSSION

Structural analysis

Scanning electron microscopy

The SEM micrographs of pure PVC and PVC composites filled with 40 wt.% micro CuO, 40 wt.% nano CuO, 40 wt.% micro PbO, and 40 wt.% nano PbO are displayed in fig. 3. Figure 3 demonstrates that there is a clear variation between the morphology of pure PVC, fig. 3(a), and CuO/PVC and PbO/PVC composites, figs. 3(b)-3(e). From fig. 3, the SEM micrographs of micro- and nano- CuO/PVC and PbO/PVC composites at 40 wt.% are compared. It is clear that, in the case of nanocomposites, the nanoparticles are dispersed uniformly and well embedded in the PVC matrix which provides an interlocking structure for shielding. However, in the case of micro composites, bulky particles are not well covered with the PVC matrix and some of them are peeled off from the matrix which acts as voids for shielding.

Field-emission transmission electron microscopy

Field-emission transmission electron microscopy (FE-TEM) micrographs of the PVC composites filled with 20 wt.% nano PbO and 20 wt.% nano CuO are shown in figs. 4(a) and 4(b) respectively. Figure 4(a), shows that PbO nanoparticles have a spherical shape with a particle size around 30 nm. In addition, fig. 4(b) shows the presence of CuO nanoparticles with an average particle size of around 15 nm.

Mechanical properties

The reason for adding inorganic particles into polymers is to improve their mechanical properties via reinforcement mechanisms as described in the literature [12, 13]. The stress-strain relationship in polymers is considered as complex dependencies and is nonlinear in nature [19]. The typical stress-strain curves of pure PVC, micro composites, and nanocomposites with a different particle content measured at room temperature and constant loading rate (3 mm per min) are displayed in fig. 5. Stiffness (determined from the slope of the linear part of the stress-strain curve up to the elastic point), the ultimate tensile strength, the yield stress, and % elongation at break are the most important tensile mechanical properties which are obtained from the test for reinforced and unreinforced polymeric materials. These tensile characteristics have been determined from the stress-strain curve and are summarized in tab. 1.

The typical stress-strain curves of the pure PVC and PbO/PVC micro composites at different filler loadings are illustrated in fig. 5(a). It can be noted that in-

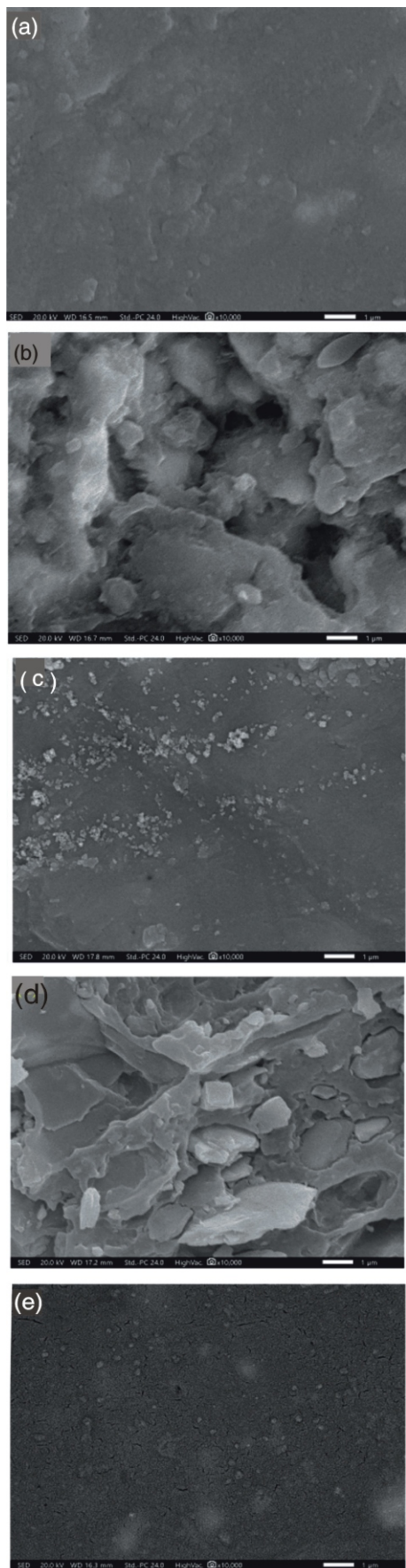


Figure 3. The SEM micrographs of (a) pure PVC, (b) 40 wt.% micro CuO /PVC, (c) 40 wt.% nano CuO /PVC, (d) 40 wt.% micro PbO /PVC, and (e) 40 wt.% nano PbO /PVC composites

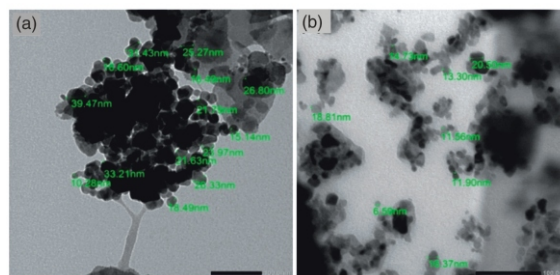


Figure 4. The FE-TEM micrographs of (a) 20 wt.% nano PbO /PVC, and (b) 20 wt.% nano CuO /PVC composites

creasing the wt.% of PbO decreases the strain while increasing the ultimate tensile strength. The curves in fig. 5(b) showed that CuO/PVC micro composites improve the stress-strain curves compared with PbO/PVC micro composites at the same wt.%. Figure 5(c) includes data of stress-strain curves of mixed (PbO + CuO)/PCV micro composites, showing the values between those of PbO/ PVC and CuO/PVC micro composites.

It is obvious from the previous data that the 40 wt.% in each figure showed better values in mechanical properties than the other wt.%, therefore, fig. 5(d) is introduced to show the comparison between their nanocomposites. From the figure, it can be seen that 40 wt.% CuO/PVC nanocomposites give the best values of mechanical properties. Also, in fig. 5, the stiffness of the composite is evaluated from the straight-line portion, whereas the other parameters like tensile strength, % elongation at break, or ultimate tensile strength, which are nonlinear mechanical properties, are evaluated at high strain [20].

Figure 6 displays the variation of yield stress, ultimate tensile strength, percent elongation at break, and stiffness of the examined composites as a function of reinforcing particle concentration. It is observed from the tab. 1 and fig. 6 that pure PVC has a higher percent elongation than the other composites filled with either micro or nanoparticles while by increasing the filler wt.% there is an increase in the values of the stiffness, ultimate tensile strength, and yield stress of the composites compared to the pure PVC and this is considered as an improvement in the mechanical properties of PVC. For PVC composites filled with PbO micro-particles, it was found that by increasing the filler wt.% there is an increase in the values of the stiffness, ultimate tensile strength, and yield stress of the composites compared to pure PVC. The data obtained in the tab. 1 about PVC composites filled with CuO micro particles showed that there was an improvement in the mechanical properties of micro CuO/PVC composites than micro PbO/PVC composites at the same wt.%. Furthermore, the mixed micro (PbO + CuO) /PVC composites have the values of mechanical properties that lie between micro PbO/PVC composites and micro CuO/ PVC composites. Also, the composite of 40 wt.% micro filler content has the highest tensile strength.

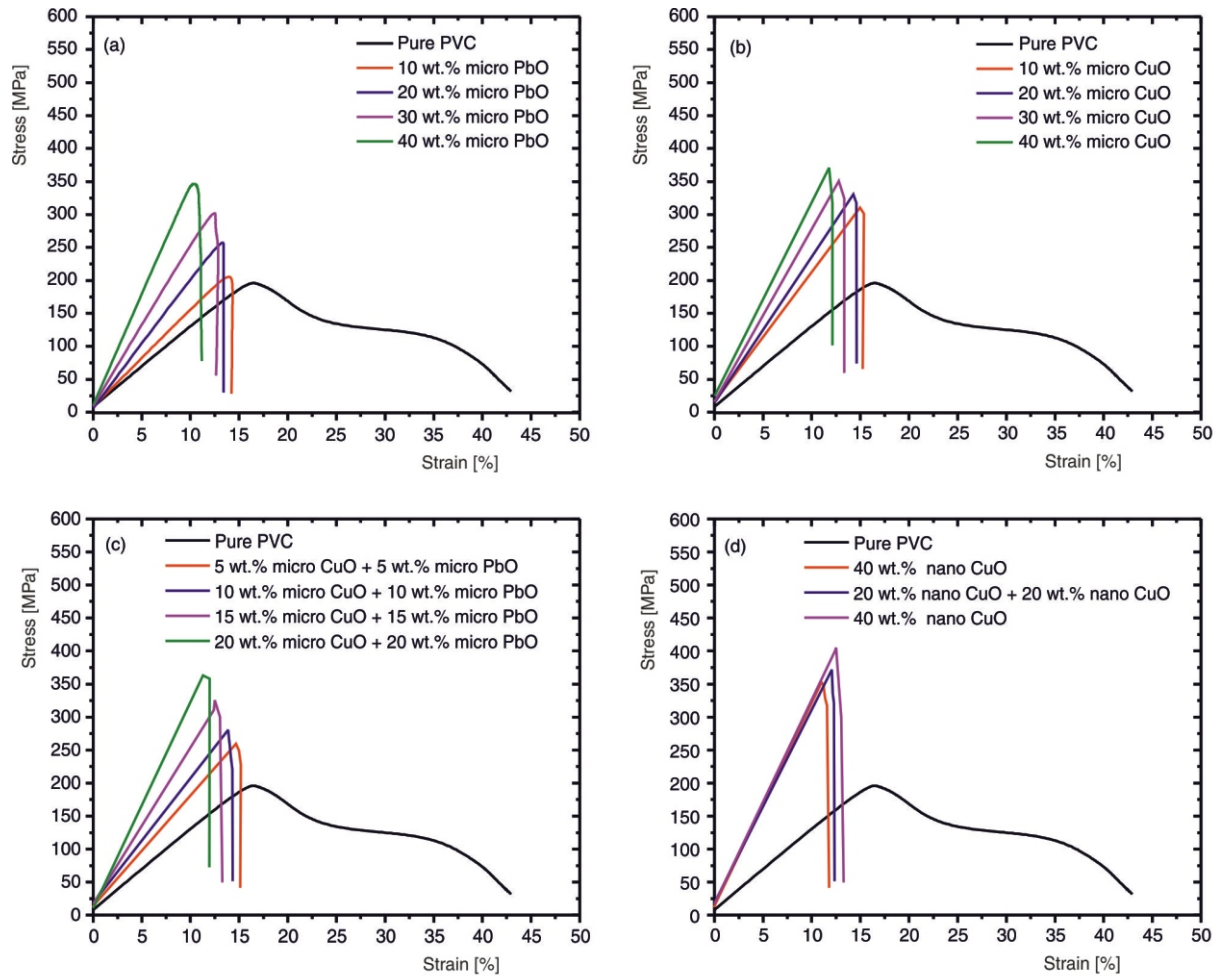


Figure 5. Typical tensile stress-strain curves of pure PVC and (a) micro PbO/PVC, (b) micro CuO /PVC, (c) micro (PbO + CuO)/ PVC, and (d) nano (PbO + CuO)/ PVC composites at different wt.%

Table 1. Mechanical properties of PbO/PVC and CuO/PVC composites

Filler [wt.%]	Yield stress (N)	Ultimate tensile strength (N)	Stiffness (N)	Elongation at beak [%]
Pure PVC	188.72 0.4	200.47 0.2	12.86 0.12	42.96 1
10 wt.% Micro PbO	207.52 0.5	219.48 0.3	14.01 0.22	14.37 3
20 wt.% Micro PbO	243.70 0.1	269.12 0.4	17.73 0.15	13.40 4
30 wt.% Micro PbO	280.83 0.4	314.01 0.4	21.65 0.33	12.84 2
40 wt.% Micro PbO	332.52 0.3	348.33 0.1	25.02 0.24	11.16 3
10 wt.% Micro CuO	300.99 0.2	310.20 0.5	18.59 0.31	15.35 2
20 wt.% Micro CuO	317.56 0.3	330.45 0.2	20.77 0.44	14.61 1
30 wt.% Micro CuO	324.53 0.1	350.44 0.2	24.65 0.28	13.33 1
40 wt.% Micro CuO	366.73 0.4	370.73 0.1	28.18 0.51	12.14 3
5 wt.% Micro CuO + 5 wt.% Micro PbO	227.98 0.5	259.46 0.3	16.90 0.21	15.18 2
10 wt.% Micro CuO +10 wt.% Micro PbO	280.63 0.3	280.64 0.4	19.21 0.32	14.35 1
15 wt.% Micro CuO +15 wt.% Micro PbO	300.58 0.1	323.50 0.1	22.65 0.42	13.29 2
20 wt.% Micro CuO +20 wt.% Micro PbO	357.92 0.2	362.96 0.5	26.51 0.24	11.93 3
40 wt.% Nano PbO	327.98 0.3	352.46 0.2	26.84 0.18	11.80 2
20 wt.% Nano CuO +20 wt.% Nano PbO	350.76 0.2	371.64 0.3	27.94 0.27	12.35 2
40 wt.% Nano CuO	400.58 0.4	405.50 0.3	31.03 0.11	13.29 3

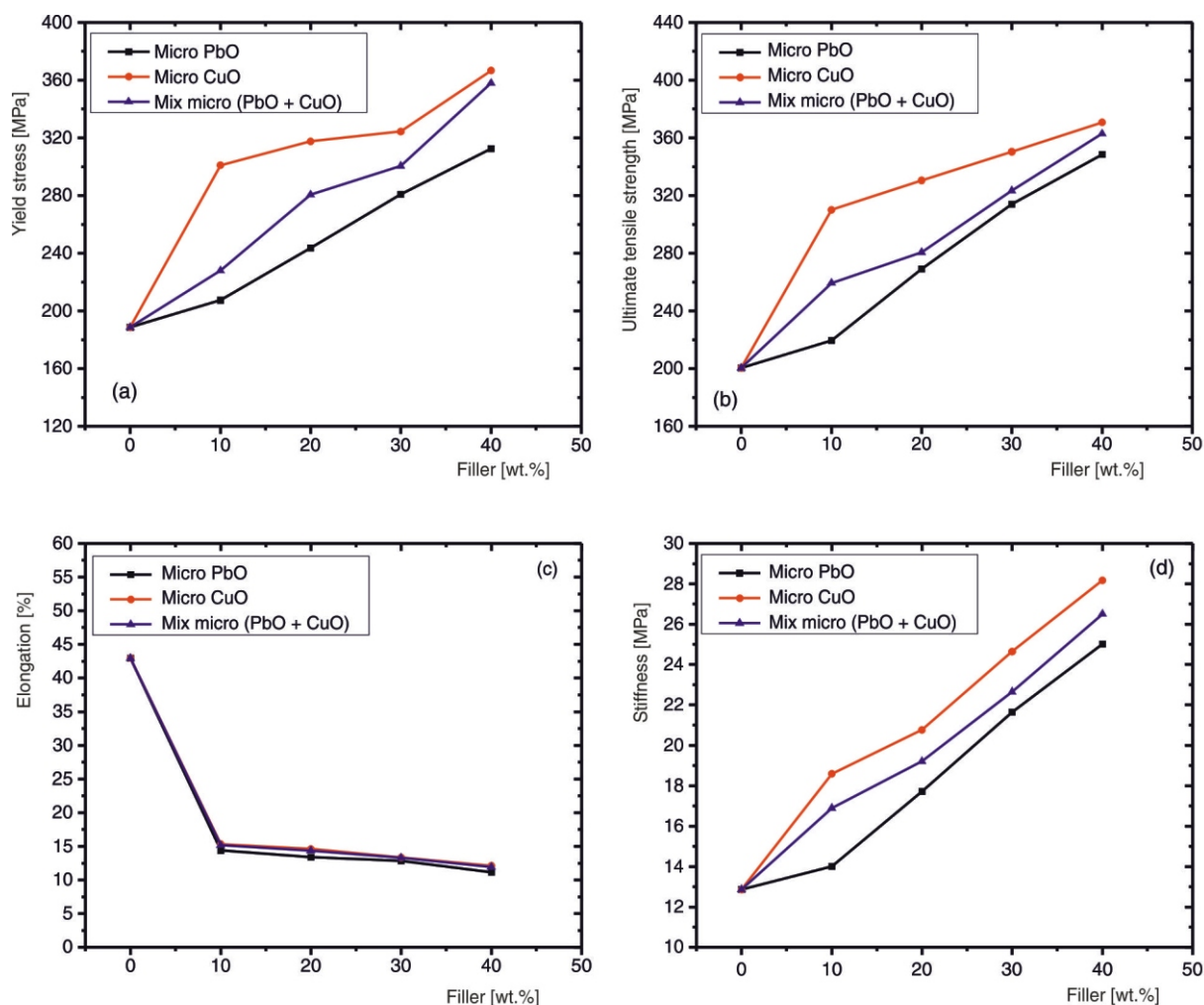


Figure 6. Effect of micro fillers on (a) yield stress, (b) ultimate tensile strength, (c) elongation at break in %, and (d) stiffness of PVC composites

Moreover, it is obvious from the tab. 1 that, the composites loaded with nanofillers show higher mechanical properties than composites loaded with bulk fillers for the same wt.%. This is attributed to the homogeneous dispersion of nanoparticles in the PVC matrix. Thus, at the same particle loading percent, the nanoparticle filler is more efficient than the bulk filler in strengthening the polymer matrix which additionally improves the mechanical properties, in other words, smaller particles give better reinforcement. Also, the composite of 40 wt.% filler content showed the highest tensile strength for both nanocomposites and micro composites which represents the optimal filler content.

Gamma-ray shielding properties of PVC composites

From spectral measurements, it was easy to graph the values of the peak areas per unit time vs. the thickness x of the composite either free or loaded with the nanoparticle PbO, CuO, or the mixture PbO +

CuO. According to the well-known formula of the Beer-Lambert law [21], the linear attenuation coefficient μ [cm^{-1}] at a particular gamma energy for each composite material was calculated by eq. (1) [22]

$$\mu = \frac{1}{x} \ln \frac{N_0}{N_x} \quad (1)$$

where N_0 is the net area at zero absorber thickness and N_x – the net area at absorber thickness x . The density of each sample was measured experimentally using the Archimedes principle [23] and is listed in tab. 2. Simply by using the values of the measured densities the mass attenuation coefficients for the investigated samples were calculated [24]. To confirm the validity of these values it was important to use the XCOM software to calculate their mass attenuation coefficients theoretically.

Table 2 clarifies both experimentally and theoretically calculated values of linear attenuation coefficients, where the theoretical values of linear attenuation coefficients were obtained by calculating the mass attenuation coefficient from the XCOM program and

Table 2. The values of the linear attenuation coefficient [cm^{-1}] and density [gcm^{-3}] for 40 wt.% CuO, 40 wt.% PbO, and mix (20 wt.% PbO + 20 wt.% CuO) micro and nano particles

Density [gcm^{-3}]	2.199 ± 0.067		2.315 ± 0.073		2.241 ± 0.018		2.323 ± 0.045	2.493 ± 0.013	2.353 ± 0.011
Linear attenuation coefficient [cm^{-1}]									
Energy [keV]	Micro particles					Nano particles			
	40 wt.% CuO	XCOM	40 wt.% PbO	XCOM	20 wt.% PbO + 20 wt.% CuO	XCOM	40 wt.% CuO	40 wt.% PbO	20 wt.% PbO + 20 wt.% CuO
59.530	1.714	1.800	4.819	4.910	2.861	2.970	2.642	5.722	3.983
80.990	0.904	0.920	2.219	2.270	1.376	1.420	1.293	2.873	1.984
121.000	1.107	1.130	3.276	3.390	1.709	1.760	1.338	4.025	2.557
244.000	0.385	0.300	0.721	0.740	0.457	0.460	0.411	0.801	0.577
343.000	0.261	0.256	0.417	0.430	0.299	0.300	0.312	0.533	0.397
356.000	0.252	0.250	0.410	0.412	0.286	0.290	0.308	0.502	0.386
661.000	0.179	0.180	0.218	0.220	0.183	0.180	0.209	0.342	0.263
776.000	0.169	0.170	0.191	0.190	0.161	0.160	0.198	0.213	0.196
960.000	0.142	0.150	0.166	0.170	0.147	0.140	0.164	0.196	0.171
1172.000	0.129	0.140	0.151	0.150	0.131	0.130	0.152	0.174	0.155
1332.000	0.119	0.130	0.137	0.140	0.123	0.120	0.137	0.146	0.134
1402.000	0.117	0.130	0.136	0.130	0.119	0.120	0.129	0.140	0.127

then multiplying by the density of the composite. It is well known that for any attenuator the values of the attenuation coefficients drop gradually with the increase in the photon's energy except in the region of the *K*-edge at low photon's energy where there is a sharp increase in the attenuation coefficients and then drops again where the predominant interaction in this region is the photoelectric effect. Anyhow, these facts illustrate the values of attenuation coefficients mentioned in tab. 2 for all the tested samples.

The variation of linear attenuation coefficients as a function of the photon's energy for micro PbO/PVC, micro CuO/PVC, and micro (PbO+CuO)/PVC composites are shown in fig. 7. The linear attenuation coefficients depend on the kind of interactions between the attenuated photons and constituents of the absorber at specific energy assumes a significant task to determine what probability will take place (photoelectric effect or Compton scattering effect, first at that point followed by a photoelectric impact) [25]. For energy less than 200 keV the most probable interactions of photons are the photoelectric effect but for photons greater than 200 keV this probability will drop strikingly with energy and the dominant interactions will be the Compton effect. In this effect in order for the photon to deposit all its energy, it must undergo numerous scattering processes that its energy diminishes to lower than 200 keV where the probability of being absorbed by the photoelectric effect is high, generally, the photon will be removed from the beam [5]. There is an important role in the interaction of photons inside the composite is the effect of the *K*-edge where the Cu has a *K*-edge at 8.9 keV [26] and that for Pb at 88 keV [27].

Figure 8 displays the Linear attenuation coefficient as a function of photon energy for 40 wt.% nano CuO/PVC, 40 wt.% nano PbO/PVC, and (20 wt.%

nano CuO + 20 wt.% nano PbO)/PVC composites compared with pure PbO and pure Pb. The examining of fig. 8 clarifies that composites loaded with nano lead oxide have the predominant effect on the attenuation of photons rather than those loaded with nano copper oxide especially in the energy region below 1 MeV but for higher energies, the values become closer. An important observation must be mentioned here that the majority of photons in this energy region will interact with the absorbing medium through Compton scattering where the photon will suffer multiple scattering to reach the region of low energy to be absorbed by the photoelectric effect or otherwise will escape from the sides of the detector. These processes are dependent on the atomic number of the absorbing medium and the energy of the photons [28]. On the other hand, to minimize the use of lead as an absorber one can replace this with composites loaded with a mixture of nano CuO and nano PbO to protect workers from the hazards of the energetic photons, besides it helps to minimize lead contaminants in the environment. The reliability in these experimental measurements could be realized from their good agreement with those determined by utilizing the XCOM program for the same composites loaded with the same percentage of nano oxides.

The half-value layer (HVL) is one of the important shielding parameters besides the attenuation coefficient, so the work is extended to calculate the HVL values for the different samples according to the simple eq. [29].

$$HVL = \frac{0.693}{\mu} \quad (2)$$

The calculated HVL values of PbO/PVC composites have been compared with that of CuO/PVC

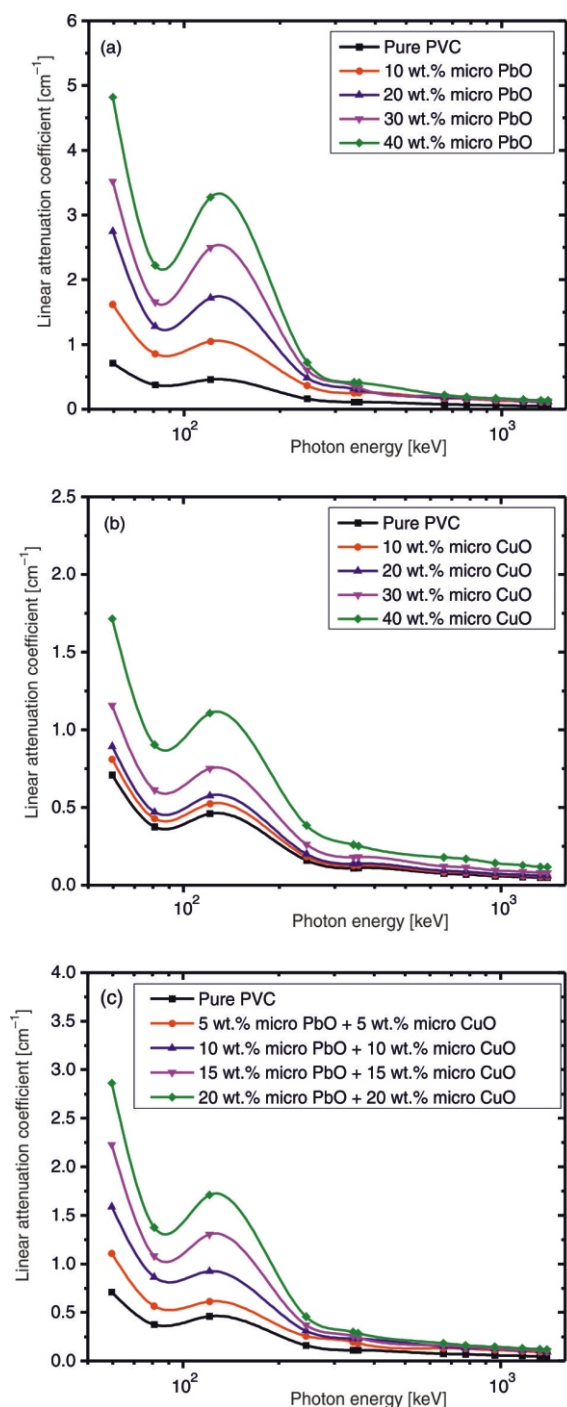


Figure 7. Linear attenuation coefficient as a function of photon energy for (a) micro PbO/PVC, (b) micro CuO/PVC, and (c) micro (PbO+CuO)/ PVC composites at different wt. %

composites and depicted in fig. 9(a) and fig. 9(b), respectively, with the same variation of percentage by weight to assess their shielding ability. The results of the HVL values of PbO/PVC and CuO/PVC composites needed to decrease the transmitted intensity to half of its original intensity show that as the energy increase the HVL values will also increase.

Figure 9(c) presents the HVL values as a function of photon energy for 40 wt.% nano CuO/PVC, 40 wt.%

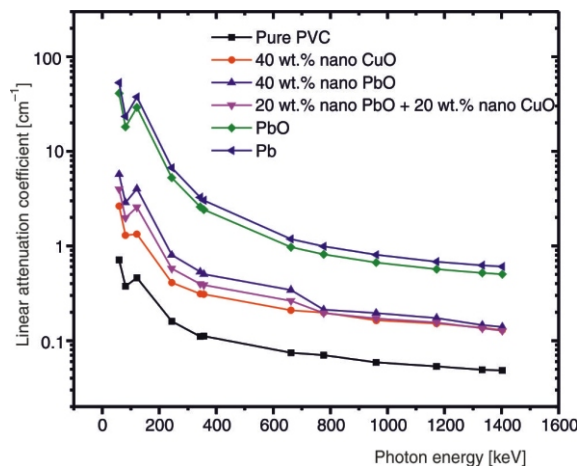


Figure 8. Linear attenuation coefficient as a function of photon energy for 40 wt.% nano CuO/PVC, 40 wt.% nano PbO/PVC, and (20 wt.% nano CuO + 20 wt.% nano PbO)/PVC composites, compared with pure PbO, and pure Pb

nano PbO/PVC, and (20 wt.% nano CuO + 20 wt.% nano PbO)/PVC composites compared with pure PbO and pure Pb. It is clear that at 40 wt. %, the HVL values for the nano-PbO/PVC and nano-CuO/PVC composites are much lower than that of micro composites at the same wt.% shown in fig. 9(a) and 9(b).

CONCLUSION

From this study, it is concluded that the composites 40 wt.% nano CuO/PVC and 40 wt.% nano PbO/PVC were selected as shielding materials due to the highest attenuation coefficients. The results of the half-thickness value show that PbO/PVC composites are preferable to CuO/PVC composites in radiation shielding protection for various radioactive sources used. On the other hand, the tensile strength and modulus of elasticity reach the highest value for the 40 wt.% CuO nanocomposite. Therefore, to minimize the use of lead as an absorber one can replace this with composites loaded with a mixture of nano CuO and nano PbO to protect workers from the hazards of the energetic photons, besides it helps to minimize lead contaminants in the environment.

AUTHORS' CONTRIBUTIONS

The experimental part was performed by O. M. Hagag and M. T. Alabsy. Theoretical analysis and writing were carried out by Y. M. Abbas, A. M. El-Khatib, and M. S. Badawi. The manuscript was conceived and prepared by all authors.

REFERENCES

- [1] El-Khatib, A. M., *et al.*, Fast and Thermal Neutrons Attenuation Through Micro-Sized and Nano-Sized

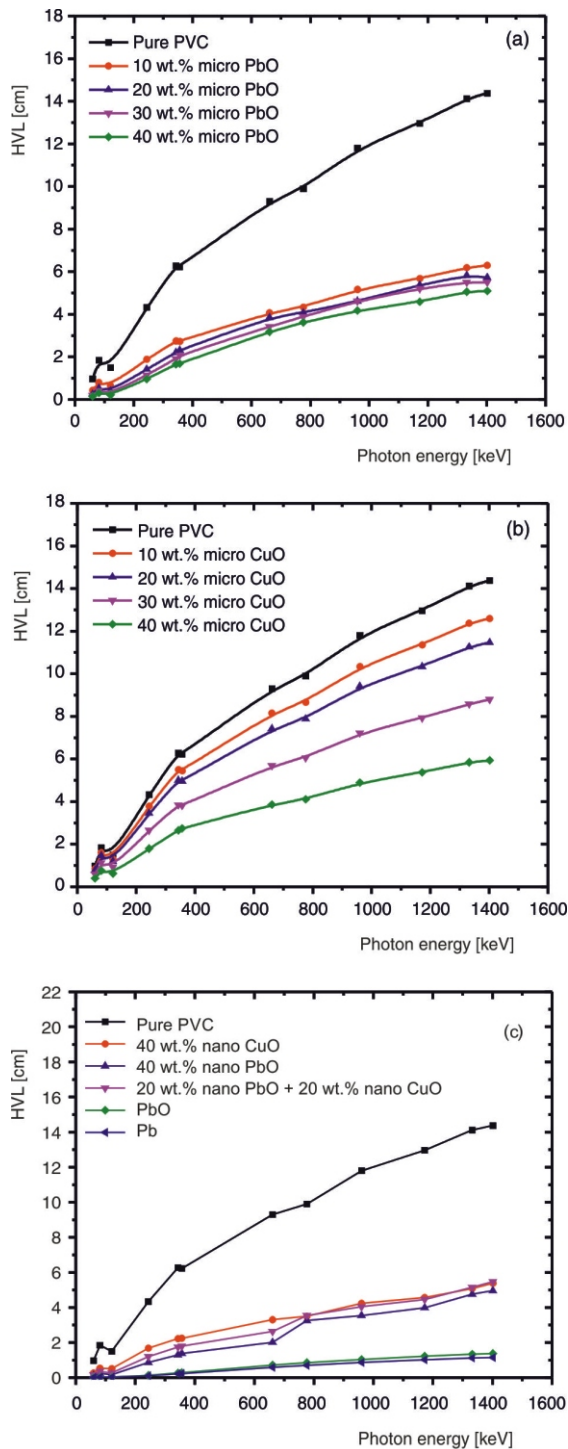


Figure 9. The HVL values as a function of photon energy for (a) micro PbO/PVC, (b) micro CuO/PVC, and (c) nano (PbO + CuO)/PVC composites, compared with pure PbO and pure Pb

- CdO Reinforced HDPE Composites, *Radiat. Phys. Chem.* 180 (2020), 109245
- [2] El-Khatib, A. M., et al., Conductive Natural and Waste Rubbers Composites-Loaded with Lead Powder as Environmental Flexible Gamma Radiation Shielding Material, *Mater. Res. Express.*, 7 (2020), 10, 105309
- [3] More, C. V., et al., Extensive Theoretical Study of Gamma-Ray Shielding Parameters Using Epoxy

- Resin-Metal Chloride Mixtures, *Nucl Technol Radiat*, 35 (2020), 2, pp. 138-149
- [4] Alharshan, G. A., et al., A Comparative Study Between Nano-Cadmium Oxide and Lead Oxide Reinforced in High Density Polyethylene as Gamma Rays Shielding Composites, *Nucl Technol Radiat*, 35 (2020), 1, pp. 42-43
- [5] El-Khatib, A. M., et al., Gamma Attenuation Coefficients of Nano Cadmium Oxide/High density Polyethylene Composites, *Sci. Rep.*, 9(2019), 1, pp. 1-11
- [6] Regnier, G., Radiation Protection, *J. Ark. Med. Soc.*, 55 (1958), 7, pp. 270-273
- [7] Singh, K., et al., Gamma Radiation Shielding Analysis of Lead-Flyash Concretes, *Appl. Radiat. Isot.*, 95 (2015), Jan., pp. 174-179
- [8] Calik, A., et al., A Comparison of Radiation Shielding of Stainless Steel with Different Magnetic Properties, *Nucl Technol Radiat*, 29 (2014), 3, pp. 186-189
- [9] Azeez, A. B., et al., Replacement of Lead by Green Tungsten-Brass Composites as a Radiation Shielding Material, *Appl. Mech. Mater.*, 679 (2014), Aug., pp. 39-44
- [10] Mehnati, P., et al., New Bismuth Composite Shield for Radiation Protection of Breast During Coronary CT angiography, Iran, *J. Radiol.*, 16 (2019), 3, e84763
- [11] Bin Aziz, M. A., et al., Comparison of Lead, Copper and Aluminium as Gamma Radiation Shielding Material through Experimental Measurements and Simulation Using MCNP Version 4c, *Int. J. Contemp. Res. Rev.*, 9 (2018), 8, pp. 20193-20206
- [12] Camargo, P. H. C., et al., Nanocomposites: Synthesis, Structure, Properties and New Application Opportunities, *Mater. Res.*, 12 (2009), 1, pp. 1-39
- [13] Zhang, X., Simon, L. C., In Situ Polymerization of Hybrid Polyethylene-Alumina Nanocomposites, *Macromol. Mater. Eng.*, 290 (2005), 6, pp. 573-583
- [14] Umer, A., et al., A Green Method for the Synthesis of Copper Nanoparticles Using L-Ascorbic Acid, *Rev. Mater.*, 19 (2014), 3, pp. 197-203
- [15] ***, Metal Tensile Test Procedure Quality Control & Lab Department, 2017, pp. 1-11
- [16] Csedreki, L., et al., Measurement of Gamma-Ray Production Cross Sections for Nuclear Reactions $^{14}\text{N}(d,p)^{15}\text{N}$ and $^{28}\text{Si}(d,p)^{29}\text{Si}$, *Nucl. Instruments Methods Phys. Res. Sect. B Beam Interact. with Mater. Atoms.*, 328 (2014), pp. 20-26
- [17] El-Khatib, A. M., et al., Full-Energy Peak Efficiency of an NaI(Tl) Detector with Coincidence Summing Correction Showing the Effect of the Source-To-Detector Distance, *Chinese J. Phys.*, 55 (2017), 2, pp. 478-489
- [18] Alsayed, Z., et al., Study of Some γ -Ray Attenuation Parameters for New Shielding Materials Composed of Nano ZnO Blended with High Density Polyethylene, *Nucl Technol Radiat*, 34 (2019), 4, pp. 342-352
- [19] Khalaf, M. N., Mechanical Properties of Filled High Density Polyethylene, *J. Saudi Chem. Soc.*, 19(2015), 1, pp. 88-91
- [20] Kim, S., et al., Multifunctional xGnP/LLDPE Nanocomposites Prepared by Solution Compounding Using Various Screw Rotating Systems, *Macromol. Mater. Eng.*, 294 (2009), 3, pp. 196-205
- [21] Yang, Z., et al., Crystallization Behavior of Poly (ϵ -Caprolactone)/Layered Double Hydroxide Nanocomposites, *J. Appl. Polym. Sci.*, 116 (2010), 5, pp. 2658-2667
- [22] Badawi, M. S., A Numerical Simulation Method for Calculation of Linear Attenuation Coefficients of Unidentified Sample Materials in Routine Gamma Ray Spectrometry, *Nucl Technol Radiat*, 30 (2015), 4, pp. 249-259

- [23] Kireš, M., Archimedes' Principle in Action, *Phys. Educ.*, 42 (2007), 5, pp. 484-487
- [24] Harish, V., et al., Lead Oxides Filled Isophthalic Resin Polymer Composites for Gamma Radiation Shielding Applications, *Indian J. Pure Appl. Phys.*, 50 (2012), Nov., pp. 847-850
- [25] El-Khatib, A. M., et al., Computation of the Full Energy Peak Efficiency of an HPGE Detector Using a New Compact Simulation Analytical Approach for Spherical Sources, *J. Eng. Sci. Technol.*, 8 (2013), 5, pp. 623-638
- [26] Gaur, A., et al., Copper K-edge XANES of Cu(I) and Cu(II) Oxide Mixtures, *J. Phys. Conf. Ser.*, 190 (2009), 1, 012084
- [27] Mesquita, A., et al., Ti K-edge XANES and Pb LIII-edge EXAFS studies of $PbZr_{0.40}Ti_{0.60}O_3$ Ferro-electric Material, *J. Phys. Conf. Ser.*, 190 (2009), 1, 012081
- [28] Hasan, W. K., et al., Measurement Technique of Linear And Mass Attenuation Coefficients of Polyester – Bentonite Composite as Gamma Radiation Shielding Materials, *AIP Conf. Proc.*, 2144 (2019), Aug., doi.org/10.1063/1.5123088
- [29] Akkas, A., Determination of the Tenth and Half Value Layer Thickness of Concretes with Different Densities, *Acta Phys. Pol. A.*, 129 (2016), 4, pp. 770-772

Received on January 10, 2021

Accepted on March 19, 2021

**Јехиа М. АБАС, Ахмед М. ЕЛ-КАТИБ, Мохамед С. БАДАВИ,
Махмуд Т. АЛАБСИ, Осама М. ХАГАГ**

ГАМА СЛАБЉЕЊЕ КРОЗ НАНО-ОЛОВО – НАНО-БАКАРНЕ ПВЦ КОМПОЗИТЕ

Полимарни композити поливинилхлорида испуњени су микро и нано честицама PbO/CuO. Додати проценат сваког масеног удела био је 10 wt.%, 20 wt.%, 30 wt.%, и 40 wt.%, уз 40 wt.% мешовитог композита (20 % CuO + 20 % PbO). Коefицијенти масеног и линеарног слабљења испитиваних композита измерени су у функцији енергије гама зрачења у распону од 59,53 keV до 1408,01 keV, користећи стандардне радиоактивне тачкасте изворе. Да би се потврдила валидност ових резултата, коefицијенти слабљења за расуте по запремини композите (PVC + PbO + PVC + CuO) израчунати су помоћу софтвера ХСОМ. Резултати су се добро слагали са вредностима добијеним експерименталним радом. Упоредивањем коefицијената слабљења различитих композита утврђено је да они који су испуњени или са нано PbO или са нано CuO имају веће вредности од оних расутих по запремини са истим процентом. Такође, узорци испуњени са нано PbO имају највише коefицијенте слабљења чак и упоређивањем са (20 wt.% CuO + 20 wt.% PbO), посебно у енергетском региону испод 1 MeV; међутим за веће енергије вредности постају врло блиске. Испитивање механичких својства таквих композита услед убризгавања по запремини, и нано метала, открива да су чврстоћа на истезање и Јангов модул PVC нанокompозитних листова знатно повећани са порастом концентрације наночестица CuO и PbO. Нанокompозит CuO показао је највеће вредности чврстоће на савијање, жилавости и чврстоће на истезање међу свим произведеним нанокompозитним плочама.

Кључне речи: поливинил хлорид, нано оловни оксид, нано бакарни оксид, карактеризација, нано олово-бакар-РVС композицији, гама зрачење, коefицијент слабљења, механичка својства